

2

3 **Cephalonia-Lefkas Transform Fault Zone**

4 **(CLTFZ) Complexity: Insights from 2015 Lefkas**

5 **earthquake sequence**

6

7

8

9

10

11 **ABSTRACT**

12

In order to define a better model for the Cephalonia-Lefkas Transform Fault Zone the sequence of 2015 Lefkas earthquake was examined. On 17 November 2015 (07:10 GMT) a major earthquake ($M_w=6.4$) occurred on the central-western part of Lefkas island. Several destructive events were located in the past in this fault zone, so an extensive seismotectonic study is feasible for that area. Manual analysis was performed using a custom velocity model that was determined for that purpose, applying the average travel-time residuals and location uncertainties errors minimization method. Several clusters belonging to the aftershock sequence were identified, whereas three are directly related to the causative fault, covering an area of about 25 km. The central one, which includes the mainshock, comprises of only a few aftershocks. The northern, within which the majority of aftershocks are located, lies in the central part of Lefkas island and the southern occurred close to the SW edge of the island. In addition, offshore clusters with distinct characteristics have been identified to the south, between Lefkas and Cephalonia islands. The temporal evolution of the aftershock sequence indicates that no migration was observed, given that after the occurrence of the mainshock the entire epicentral area was activated. Focal mechanisms of the Seismological Laboratory of the University of Athens showed dextral strike-slip faulting for both mainshock and major aftershocks of the sequence. Taking into account the spatial distribution of the aftershocks, supported by the tectonic and geomorphological settings of the region, a deformation pattern, consisting of the Cephalonia-Lefkas and Ithaca-Lefkas major fault zones which converge in the area of Vassiliki bay is proposed. The appearance of the southernmost clusters was interpreted by the positive Coulomb stress changes transfer due to major earthquake $M_w=6.4$.

13

14 *Keywords: [Seismotectonic analysis; releasing bends; restraining bends; Lefkas aftershock*

15 *sequence; Western Greece]*

16

17

18

19

20

21 **1. INTRODUCTION**

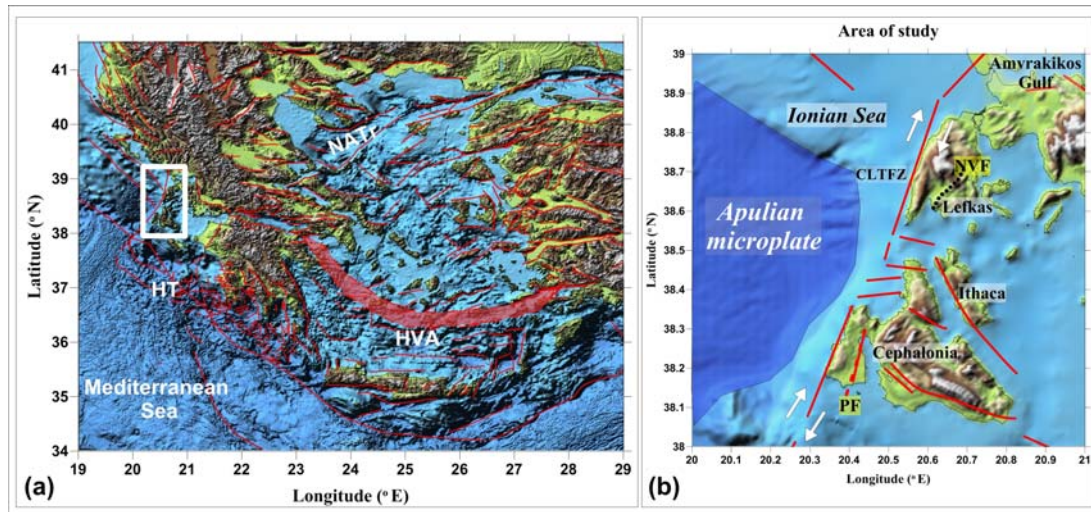
22

23 The Hellenic peninsula is bounded by important geologic and tectonic features such as the

24 Alpine mountain chain to the North, caused by the collision between Europe and Africa [1],

25 the North Anatolian Fault zone to the East [7][10][32][33][34], created by the lateral motion of

26 Anatolia with respect to the European tectonic plate [2] and the Hellenic arc to the south,
27 characterized by the subduction of Tethys oceanic crust [43].



28

29 **Fig. 1. a) Main tectonic and volcanic elements of the broader area of Greece**
30 **[9][17][31]. The study area is highlighted with a white rectangle b) Zoom in the study**
31 **area of Central Ionian Sea, showing the islands of Cephalonia and Lefkas.**
32 **Abbreviations in both maps are as following: HT, Hellenic Trench; NATr, North**
33 **Aegean Trough; HVA, Hellenic Volcanic Arc; CLTFZ, Cephalonia-Lefkas Transform**
34 **Fault Zone; PF, Paliki Fault; NVF, Nydri-Vassiliki Fault.**

35 The area of Western Greece (Fig. 1.) which is running from the Greek-Albanian borders to
36 the southern edge of Peloponnese and from the Ionian Islands to eastern Thessaly and
37 Macedonia lies between a continental collision zone to the north (Adria Microplate-Eurasia)
38 and the Hellenic Trough to the south, where remnants of the Eastern Mediterranean oceanic
39 crust subduct under the Aegean continental lithospheric microplate. These zones are linked
40 with the Cephalonia-Lefkas Transform Fault Zone (CLTFZ), playing an important role in the
41 geodynamics of the area. Seismological data for the CLTFZ indicate right-lateral strike-slip
42 focal mechanisms [37] [30] which is in agreement with the geodetic data revealing the NNE-
43 SSW direction of slip motion [13] [23]. The seismic strain rate is well correlated with the
44 principal horizontal axis of the total geodetic strain rate field. Some smaller neotectonic
45 structures are mainly expressed by minor faults that strike NNE-SSW to E-W direction,
46 overprinting the pre-existing thrust-related Plio-Quaternary features, breaking up the island
47 in multiple independent fault blocks [24].

48 The broader area of study is characterized by a series of NW-SE striking geotectonic units,
49 such as the Pre-Apulian (or Paxos) and Ionian [12], forming the External Hellenides terrain.
50 These structures which have resulted by a subduction-related compressional regime are
51 coaxial with earlier Alpine ones resulting from the collision of the Pre-Apulian plate with
52 Eurasia. The mountain chain of Hellenides located between southern Albania and the Gulf of
53 Corinth plays an important role on the seismotectonics of the region.

54 The Ionian Islands are separated from the mainland by rapidly extensional Pliocene-
55 Quaternary basins [5] [45]. The oldest sediments that fill those basins are of Pliocene age. In
56 Lefkas Island, carbonate and clastic sediments of the Hellenic arc external geotectonic units

57 dominate the geological setting [35]. The geotectonic units of Paxos and Ionian are
58 separated by a major west-directed thrust [3] [12], marked by Triassic evaporitic domes [14].

59 The majority of strong earthquakes in the broader region have mainly occurred along the
60 main tectonic features, such as the CLTFZ. Lefkas Island is characterized by the occurrence
61 of large earthquakes, both during the historical and the instrumental era, causing significant
62 damage [27] [38]. Most events were located close to the NW part of the island. More
63 specifically, the 22 November 1704 (M=6.3), the 12 October 1769 (M=6.7), the 23 March
64 1783 (M=6.7), the 28 December 1869 (M=6.4) and the 27 November 1914 (M=6.3)
65 earthquakes were among the most significant ones. They caused several deaths, injuries,
66 collapse of buildings, fissures, liquefactions and landslides at the northwestern and central
67 parts of the island. This is the reason why most epicenters of the historical earthquakes are
68 located close to the northern end of the CLTFZ, in the Ionian Sea [21] [26]. More recently, on
69 14 August 2003 (05:14 GMT), a large earthquake (Mw=6.3) with a focal depth of 9 km
70 occurred close to the NW coast of Lefkas Island [3] [44] [29].

71 On the other hand, only two large events have been located close to the southwestern edge
72 of the Lefkas Island, an area that belongs to the central part of the CLTFZ. Nevertheless,
73 important microseismic activity is observed. The two events, related to this area, are the 22
74 February 1723 (M=6.7) and the 22 April 1948 (M=6.5) earthquakes. Concerning the latter
75 event, it caused damage at the SW part of the island, while fissures and tsunami waves
76 were also observed. Two months later, on 30 June 1948, an earthquake of magnitude M=6.4
77 occurred at the NW part of the island.

78 A strong earthquake of moment magnitude Mw=6.4 occurred on 17 November 2015 at the
79 western part of Lefkas Island, causing some damage, landslides and ground fissures. In the
80 present study, this earthquake sequence is investigated in detail. For that purpose, precise
81 hypocentral locations are required. The latter were obtained using a local velocity model that
82 is determined in this study.

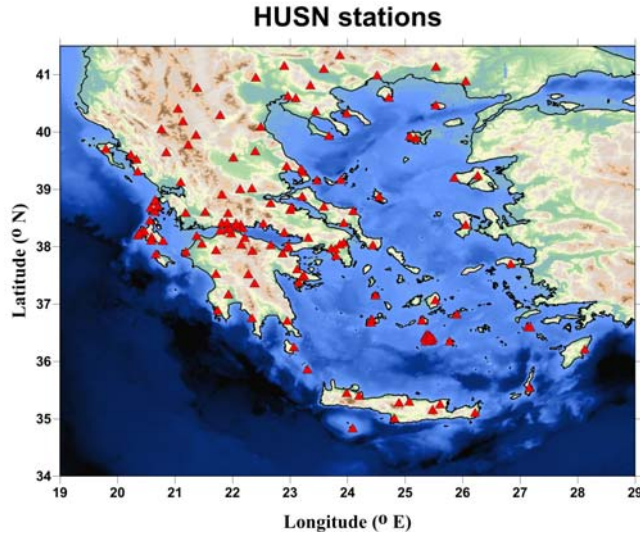
83

84 **2. DATA AND METHODS**

85

86 The present study focuses in the area of Central Ionian Islands (Western Greece), where
87 data of several local stations belonging to the Hellenic Unified Seismological Network
88 (HUSN) [8] were used for the construction of the local 1D velocity model. HUSN (Fig. 2.)
89 comprises stations from the Seismological Laboratory of the University of Athens (S.L-
90 U.O.A), the Geodynamics Institute of the National Observatory of Athens (GE.IN.-N.O.A),
91 the Geophysical Laboratory of the University of Thessaloniki (G.L.-A.U.TH) and the
92 Seismological Laboratory of the University of Patras (U.P.S.L.).

93 The data set used in this study comprises of more than 10,000 earthquakes which were
94 obtained from the seismological stations of HUSN and correspond to the time period 2012-
95 2017 (Fig. 2). More specifically, all the event locations were calculated using manually
96 picked P- and S-wave arrival-times, the HYPOINVERSE algorithm [18] a regional 1-D
97 velocity model, while the duration magnitude was calculated according to the formula
98 described by relevant studies [18] [30]. A subset of the data catalogue corresponds to the
99 Paliki (2014) and Lefkas (2015) earthquake sequence, in the vicinity of CLTFZ.



100

101 **Fig. 2. Distribution of HUSN stations (red triangles) throughout Greece**

102

103 **2.1 CONSTRUCTION OF LOCAL VELOCITY MODEL**

104

105 In the present study, the best located events were used to obtain an accurate local 1D
 106 velocity model for the broader area of Lefkas Island. The initial earthquake locations for the
 107 area of Western Greece were obtained using the regional velocity model derived by [17].
 108 The selected events had at least fourteen (14) P- and eight (8) S-wave arrival times. The
 109 present model was determined by applying the average travel-time residuals and location
 110 uncertainties errors (RMS, ERX, ERY, ERZ) minimization method [19] [6] [25]. The obtained
 111 local velocity model (Table 1) yielded improved hypocentral solutions with smaller errors
 112 than those derived by the initial one (Table 2).

113 **Table 1. Regional and custom velocity model**

Layer	Karakonstantis (2017) $V_p/V_s=1.79$		This Study $V_p/V_s=1.79$	
	V_p (km/s)	Depth (km)	V_p (km/s)	Depth (km)
1	5.3	0.0	4.9	0.0
2	6.0	6.0	5.2	4.0
3	6.3	11.0	5.9	7.0
4	6.5	14.0	6.2	11.5
5	6.7	21.0	6.4	13.0
6	7.3	39.0	6.5	16.0
7	8.0	80.0	7.3	39.0

114

115 The value of V_p/V_s ratio was obtained using the following methods: a) Chatelain (1978), that
 116 consists of determining the slope of the straight best-fit line of the difference between S-
 117 wave and P-wave travel-times for each couple of stations and for each event and b) the
 118 travel-time residuals and location uncertainties errors (RMS, ERX, ERY, ERZ) minimization
 119 method. The last mentioned V_p/V_s ratio determination method follows the same procedure
 120 that was performed in order to define velocity and ceiling depth for each layer. The data for
 121 both Chatelain and Spatio-Temporal Error Minimization methods converge to the same
 122 V_p/V_s ratio value of 1.79. Error statistics for all spatial groups with both regional and custom

123 local models are presented in Table 2. The mean horizontal (ERH) and vertical (ERZ)
124 location errors of the events located in the broader study area are smaller than 1 km, while
125 the mean RMS error is 0.132 sec.

126 **Table 2. Statistics of location uncertainties and median depth for the regional**
127 **and custom model**

	Karakonstantis (2017)	This Study
Mean RMS (s)	0.139	0.132
Median RMS (s)	0.110	0.110
Mean ERH (km)	1.125	0.909
Median ERH (km)	0.730	0.580
Median ERX (km)	0.510	0.380
Median ERY (km)	1.070	1.050
Mean ERX (km)	0.614	0.459
Mean ERY (km)	1.636	1.360
Mean ERZ (km)	1.933	1.323
Median ERZ (km)	1.310	0.870
Mean Depth (km)	7.542	8.765
Median Depth (km)	6.860	8.375
St.Dev.Y (km)	13.036	13.076
St.Dev.X (km)	6.569	5.963
St.Dev.Z (km)	3.550	3.459

128

129

130

131

2.2 COULOMB STRESS TRANSFER

132

133

134

135

In order to investigate the possible acceleration or triggering of the above-observed clusters due to the strong earthquake $M_w=6.4$, the Coulomb stress changes transfer was calculated in different depths and cross-sections. The transferred ΔCFF was determined on the fault plane with an effective coefficient of friction $\mu=0.4$ [39] [40].

136

137 **3. RESULTS AND DISCUSSION**

138

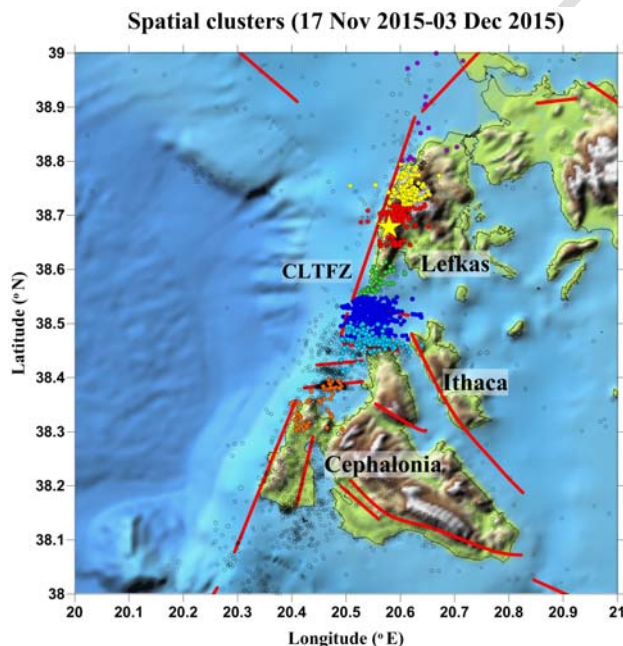
139 On 17 November 2015 (07:10 GMT) a destructive earthquake occurred along the SE coast
140 of Lefkas Island, in the vicinity of Athani village. There were two fatalities, one due to rockfall
141 and one caused by a paddock collapse. Eight people were injured, two of which children.
142 Certain collapses, rockfalls and landslides have been reported.

143 Manual analysis was conducted for the mainshock and for more than 2,500 aftershocks for
144 the period between 17 November and 3 December 2015, during which the major part of the
145 ruptured area was activated. Thus, it is considered that this period provides all necessary
146 information to interpret the 2015 Lefkas seismic sequence.

147 **3.1 Description of clustered seismicity**

148

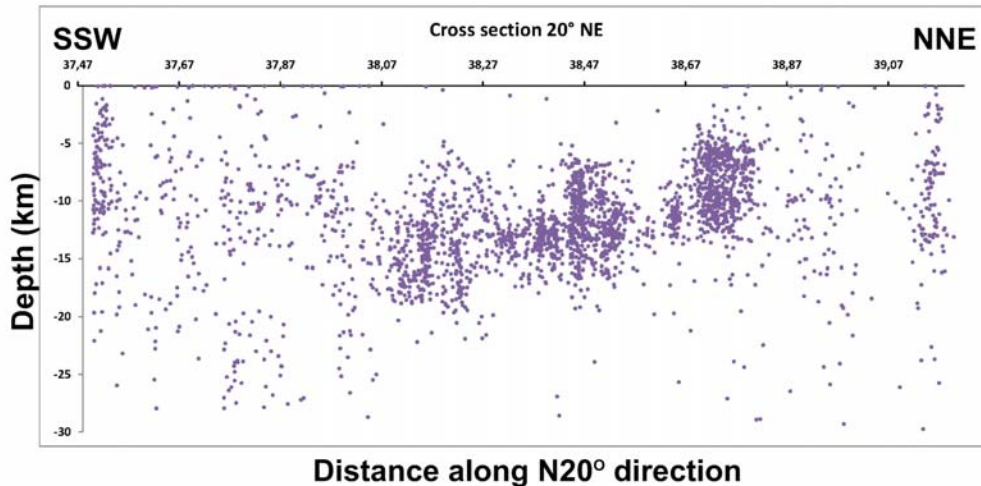
149 The hypocentral locations, using the newly developed 1-D local velocity model, revealed that
150 the aftershock sequence mainly occurred in the mid-western part of Lefkas Island. However,
151 another group of events is located S of Lefkas Island, offshore, towards Cephalonia Island. It
152 is worth noting that the largest aftershock ($M_w=5.0$) occurred near the mainshock, on 17
153 November 08:33 UTC. Both mainshock and the largest aftershock of 17 November 2015 are
154 well aligned in a SSW-NNE direction. Several linear structures can be distinguished, many of
155 which offshore, south of Lefkas island, trending roughly E-W. The aftershock distribution
156 appears mostly aligned in a $N20^\circ E$ direction with several branches oriented $\sim N30^\circ E$,
157 including the northernmost and southernmost tips (Fig. 3.).



158

159 **Fig. 3. Map of the study area showing the seven (7) main spatial clusters marked with**
160 **different colors: cluster #1 (orange), cluster #2 (cyan), cluster #3 (blue), cluster #4**
161 **(green), cluster #5 (red), cluster #6 (yellow) and cluster #7 (purple). The back ground**
162 **seismicity, before and after the main body of the aftershock sequence is marked with**
163 **grey open circles.**

164 The cross-section drawn at N20°E (Fig. 4.), roughly parallel to the CLTFZ, indicates that the
 165 total length of the activated area is approximately 60 km. The focal depths are distributed
 166 between 5 and 15 km, with the clusters in the northern group (5 - 7) being generally
 167 shallower than those of the southern group (1 - 4). The mainshock, as well as the strongest
 168 aftershock (Mw=5.0) of 17 November are contained in cluster #5.



169

170 **Fig. 4. SSW-NNE cross-section of the main body of the aftershock sequence. Top axis**
 171 **is marked by the values of latitude (°N) that the thin section passes by.**

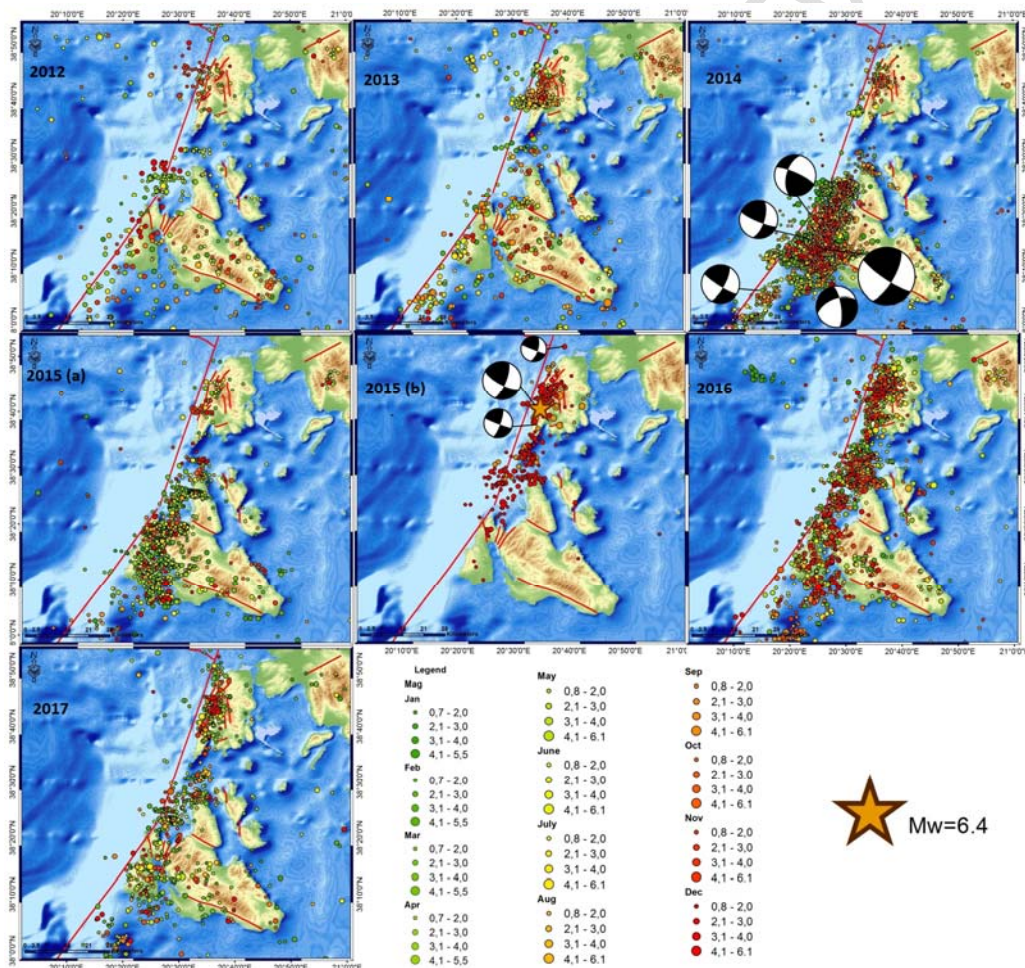
172 The epicenter of the major events of this cluster are mainly aligned SSW-NNE, with the
 173 smaller sub-cluster being apparently oriented E-W near Vassiliki bay. By far the largest
 174 cluster is #6, which contains more than 100 events of the aftershock sequence (17/11/2015-
 175 03/12/2015). Cluster #6 is divided into two branches in its shallower parts (4-6 km), one
 176 SSW-NNE, similar to cluster #5, and another trending WSW towards the western coast,
 177 extending a bit deeper (8-9 km) ENE. The described hypocentral distribution is probably
 178 related to fault network complexity, which has possibly acted as a barrier, prohibiting the
 179 main rupture to extend further north. It also contains most of the major aftershocks (13
 180 events with $M_w \geq 3.9$) which are, on average, located at slightly larger focal depths (~10 km)
 181 than the smaller ones (~6 km). Further north, cluster #7 extends ~17 km and deepens from
 182 ~6 km onshore (excluding a few sparsely located shallower events) down to ~15 km and
 183 includes the second largest aftershock (Mw=5.0) which occurred on 18 November 2015,
 184 12:15 UTC. The cluster could be further divided in 2 sub-clusters, the one for the shallower,
 185 roughly onshore events, trending S-N and the other, offshore further north, containing fewer
 186 events and apparently trending SW-NE.

187 At the southern group, the northern tip of cluster #4 is ~4-5 km south of the mainshock and
 188 the cluster extends about 8 km SSW while its median focal depth (~12 km) is larger than the
 189 one for cluster #5 (~9 km). It probably belongs to the same fault plane as the one of the main
 190 rupture and defines its deeper seismogenic part. Clusters #2 and #3 are less dispersed than
 191 cluster #4 and their distribution is roughly oriented E-W. Cluster #2, in particular, contains 2
 192 large sub-clusters at 8 – 13 km depth and a smaller sub-cluster at 15 km depth. The
 193 southernmost cluster #1 is a bit offset from the cross-section line (Fig. 4). Its main body is
 194 located at 7-9 km depth and it also includes several sub-clusters dispersed further south.
 195 At the very southern edge of the study area, a group of 3 deeper events at ~23-24 km, with
 196 epicenters between Ithaki and Cephalonia islands, are also included in cluster #1.

197 The Lefkas 2015 aftershock sequence is typical in terms of its spatio-temporal
 198 characteristics. Aftershocks were generated at both northern and southern edges of the
 199 zone within minutes to hours following the mainshock, as it is evident from S.L-U.o.A
 200 catalogue (http://www.geophysics.geol.uoa.gr/stations/gmaps3/leaf_significant.php?mapmode=mec&lng=en&year=2015#mapanc) while the largest one (Mw=5.0) occurred in less than
 202 2 hours after the main event, in the same cluster. By the end of December 2015, the activity
 203 in most of the spatial groups had diminished (Fig. 5), with the exception of cluster #6, and
 204 the sequence was typically over, as confirmed by routine observations of the seismicity rate
 205 during the following months.

207 3.2 Focal Mechanisms

208
 209 Fault plane solutions of the largest aftershocks (Mw≥5.0), determined by the Seismological
 210 Laboratory of the University of Athens (S.L-U.o.A; <http://www.geophysics.geol.uoa.gr>),
 211 indicate dextral strike-slip faulting. As an example, the focal mechanism of the largest
 212 (Mw=5.0) aftershock, occurred on 17 November 2015 (08:33 GMT), 4 km SSW of the
 213 mainshock, is presented in Fig. 5.



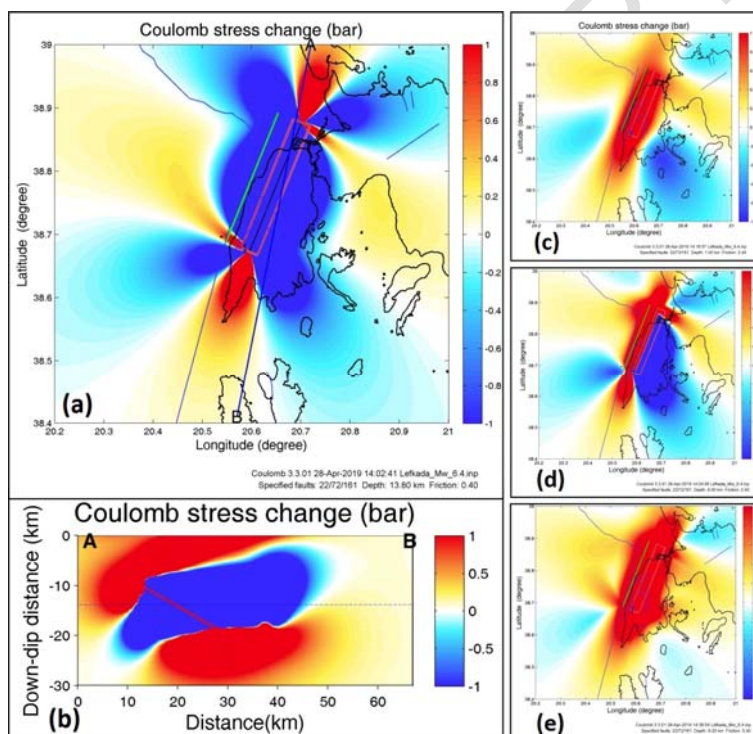
214
 215
 216

Fig. 5. Evolution of the seismicity in the study area before (2012-2015a) and after (2015b-2017) the occurrence of November 17, 2015 M6.4 Lefkas earthquake.

217 Focal mechanisms revealed the activation of an almost vertical right lateral strike slip fault, in
 218 agreement with the ENE-WSW oriented CLTFZ. The obtained results indicate that the
 219 dimensions of the activated fault, located between the main aftershock cluster in the central
 220 part of the island and the respective one SSW of Lefkas, are 25 km length and 10 km width.
 221 The focal mechanisms of the events located offshore, between Lefkas and Cephalonia
 222 Islands, are similar to the respective solution of the mainshock. Nevertheless, taking into
 223 account additional characteristics, such as the spatial distribution of the aftershocks and the
 224 shallower bathymetry, both planes of the focal mechanism of the offshore events could be
 225 considered as the activated fault, as it will be discussed in more detail in the following
 226 section.

227 3.3 Coulomb Stress Transfer results

228
 229 The Δ CFF distribution, as well as the cross section parallel to the fault, is presented in figure
 230 6a and 6b respectively. The Coulomb stress distribution showed that the earthquake with
 231 magnitude $M_w=6.4$ caused strong positive stress changes transfer in the directions NNW
 232 and SSE, (Fig. 6c.) as well as in the upper layers from the depth of 8Km until the surface
 233 (Fig. 6d.). Additionally, the max stress coulomb values were calculated for a depth range 0-
 234 20Km with step 2Km (Fig. 6e.). The results lead to the conclusion that the southernmost
 235 clusters are triggered due to the positive Coulomb stress transfer during the fault rupture
 236 which occurred on the central-western part of Lefkada island, on 17 November 2015,
 237 ($M_w=6.4$). It is worth noting that the same procedure was observed for the 2003 Lefkas
 238 rupture process [29].



239
 240
 241 **Fig. 6. Distribution maps of Coulomb stress changes (Δ CFF) due to the 2015**
 242 **earthquake $M_w=6.4$ at the focal depth (a) and cross section AB for strike $10^\circ N$ (b).**
 243 **Δ CFF Maps for depths 1Km (c), 7Km (d), respectively. Max values of Coulomb stress**
 244 **changes for depth range 0-20Km (e).**

245

246

247

248

249

250

251

252

253

254

255

256

257

258

259

260

261

262

263

264

3.4 Discussion

The 2015 Lefkas aftershock sequence is characterized by the existence of several clusters. However, the spatial distribution of the sequence revealed the activation of a large area that extends further than the mainshock's rupture length. Its first characteristic is that only few aftershocks are located in the vicinity of the epicenter. On the contrary the most important cluster is situated at the central part of the island. It is characterized by high concentration of events, constituting the main cluster, and it is observed towards the northern end of the activated fault segment, at the mid-northern part of Lefkas Island. In the same area, an important cluster occurred during the 1994 sequence, as described by [27]. More specifically, on 29 November 1994 a moderate event of $M_w=5.1$ took place on the northern part of CLTFZ, close to the west coast of Lefkas Island, followed by a $M=4.8$ aftershock on 1 December 1994. Aftershock activity was concentrated in the west-central part of the island, in the region where the main cluster of the 2015 sequence occurred. In addition, the 1994 sequence was characterized by an almost vertical distribution, reaching 12 km depth [27]. The above-mentioned observations suggest that this area produces a complex seismicity pattern, which is probably due to the existence of a local minor fault system. This is supported by the high seismic rates, observed in the central part of Lefkas Island following the occurrence of moderate or large local events.

265

266

267

268

269

270

271

272

273

274

275

276

277

278

279

280

In addition, spatially clustered seismic activity occurred to the south, close to the NNW part of Cephalonia Island, probably is not directly related to the main activated fault since they are not located along the CLTFZ but they are shifted eastwards forming a step over of the ruptured zone. The southern clusters (#1, #2 and #3) are stretched in a roughly WNW-ESE direction, separated by gaps between them, possibly indicating the existence of small parallel left-lateral structures, transverse to the main CLTFZ. Another couple of small clusters of undefined geometry are located near the southern coast of Lefkas Island (spatial group #4). Other than that, the vicinity of the mainshock's hypocenter is characterized by few sparse aftershocks. The area defined by the spatial groups #5 and possibly #4 is considered to be the main rupture area, likely a barrier that left a few unbroken asperities where the seismic clusters are observed. However, certain clusters occurred to the south, between Lefkas and Cephalonia Islands. Taking them into account, the spatial distribution spans roughly ~60 km in a SSW-NNE direction, while focal depths vary between 5 km (mostly onshore) and 15 km (offshore). The temporal evolution of the aftershock sequence is generally smooth. No significant migration patterns were observed, as almost the full extent of the aftershock zone was activated within the first 24 hours after the mainshock.

281

282

283

284

285

286

287

288

289

290

291

292

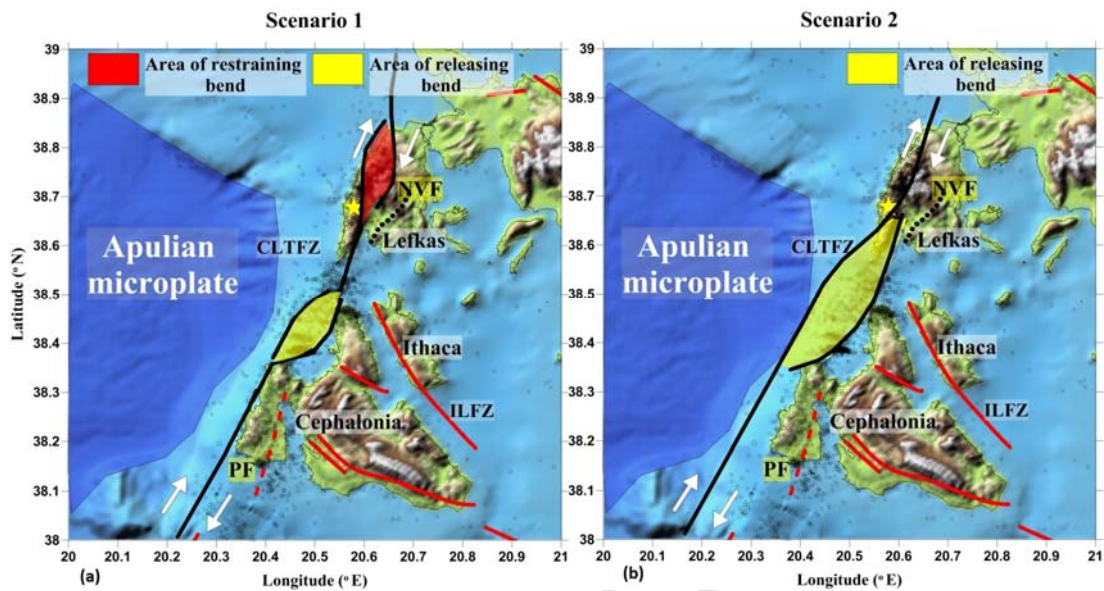
293

294

295

Recent seismotectonic studies suggest that either the CLTFZ in this area is collinear with its northern segment west of Lefkas, while further south it is shifted by some kilometers to the west of Cephalonia coast due to a transfer zone of extensional step overs [8] [13] or that the CLTFZ does not consist of a single dextral strike-slip fault, but rather a system of faults. Even though the 2015 Lefkas aftershock sequence was mainly distributed in the northern segment of the studied fault zone, some significant spatial clusters to the south of Lefkas Island appeared almost perpendicular, in a mean WNW-ESE direction, with the focal mechanisms implying sinistral strike-slip faulting. The results of the present study are in general fairly correlated to the scenario of previous seismological studies in the area [14], with the exception of the smaller than expected, according to their model, fault's dimensions, taking into account the southern clusters of the 2015 Lefkas sequence. Thus, the perpendicular secondary fault system of the latter model has to be prolonged towards the north, up to the southern part of Lefkas. In that case, the negative flower structure model, proposed by [14], could be adjusted by making a double left-bend which explains lots of the superficial geological and geomorphological features at the SW edge of Lefkas [24] [28] [2]

296 [41]. The advantage of this model is that it explains the observed seismicity south of Lefkas,
 297 while its disadvantage is the steep bending of the main part of the fault zone which is not
 298 compatible with the rupture process of the mainshock (Fig. 7a.).



299

300 **Fig. 7. a) Double left-bend of CLTFZ model (scenario 1) and b) two major converging**
 301 **fault zones (CLTFZ and ILFZ), forming an almost antithetic system of strike-slip faults**
 302 **(scenario 2).**

303

304 Another scenario, which fits most of the results obtained by this study, is combined with
 305 previous knowledge based on GPS measurements [36], geophysical [22] geomorphological
 306 and tectonic elements at the southern part of Lefkas and the sea-bottom of Myrtos Gulf [24]
 307 [41]. It includes two major fault zones, the CLTFZ and Ithaca-Lefkas (ILFZ), converging in
 308 the area of Vassiliki bay forming en-echelon arrays of WNW-ESE minor faults and
 309 fractures, separated by smaller NE-SW strike-slip faults in between (Fig. 7b), such as the
 310 one of Nydri-Vassiliki (NVF). In this model, there is the major NNE-SSW striking CLTFZ
 311 offshore, which makes a right bend NW of Myrtos bay, forming a releasing bend in a region
 312 SSW of Lefkas Island, as in California's deformation model described by [42]. On the other
 313 hand, the NNW-SSE ILFZ and CLTFZ converge in western Lefkas Island, forming an
 314 antithetic system of strike-slip faults to the overall sense of the zone's shear, comprising
 315 crustal rotated blocks of oblique minor faults in the area between Cephalonia and Lefkas
 316 Islands (Fig. 7b.).

317

318

319

320

321

322

323

324

325

326

327

4. CONCLUSION

The 17 November 2015 Mw=6.4 Lefkas earthquake is located at the southwestern part of
 the island and can be considered as the continuation of the 2003 ruptured area, which
 probably left an unbroken patch. It is obvious that the recent event occurred within this
 asperity. Taking into account both events, the activated area, with a length of about 45 km in
 a SSW-NNE direction, covers the northern part of CLTFZ that is located west of Lefkas. This
 observation implies that the accumulated energy was released in two separate events
 instead of one, which would obviously have considerably larger magnitude. Such earthquake

328 sequences, consisting of more than one event, have been reported since the historical
329 times, as in the case of the earthquakes that occurred during 1948 [27].

330 The main characteristic of the sequence is that only a few aftershocks with $M \geq 3.0$ are
331 located close to the mainshock's epicentre, suggesting that during the rupture process, no
332 unbroken patches were left at the central part of the activated fault. The southern part of the
333 activated fault, reaching the SW edge of Lefkas Island, is characterized by low seismicity.
334 Concluding, the total length of the causative fault is of the order of 25 km, while the
335 seismicity belonging to the southern and northernmost (1-3 and 7) clusters is probably not
336 directly related to the CLTFZ. The length of the total activated area is about 60 km, much
337 larger than the expected rupture length for a $M_w=6.4$ mainshock. This observation suggests
338 that the clusters #1, #2, #3 and #7 have been triggered by stress-transfer.

339 The majority of the determined focal mechanisms are similar, related to dextral strike-slip
340 faulting that was also revealed for the two earthquakes that occurred in Cephalonia during
341 January – February 2014 [30]. The events located close to Lefkas Island are related to the
342 main tectonic feature of the area, which is the Cephalonia-Lefkas Transform Fault Zone,
343 along which other significant earthquakes occurred in the past, such as the 1983 Cephalonia
344 earthquake. According to the results of the present study, the ruptured fault, with a length of
345 approximately 25 km, is the prolongation of the 2003 Lefkas earthquake causative fault.

346 The occurrence of the 2015 Lefkas earthquake sequence provided the opportunity to obtain
347 a more detailed deformation pattern, especially for the area between Lefkas and Cephalonia
348 islands. For that purpose, two major scenarios are investigated. The first is a negative flower
349 structure model prolonged towards the southern part of Lefkas. The other scenario includes
350 the Cephalonia-Lefkas and the Ithaca-Lefkas major fault zones, converging in the area of
351 Vassiliki bay, separated by smaller strike-slip faults in between, almost perpendicular to the
352 CLTFZ. Considering the second scenario, both the WNW-ESE clustered seismicity, between
353 the islands of Cephalonia and Lefkas, and the uplift region in the SW part of Lefkas Island,
354 can be reasonably explained.

355

356 **COMPETING INTERESTS**

357

358 "Authors have declared that no competing interests exist."

359

360

361

362

363

364 **REFERENCES**

365

366 1. Anderson H, Jackson J. Active tectonics of the Adriatic Region. *Geophysical Journal of*
367 *the Royal Astronomical Society*, 91: 937-983. 1987;doi:[10.1111/j.1365-246X.1987.tb01675.x](https://doi.org/10.1111/j.1365-246X.1987.tb01675.x)

368 2. Bathrellos G, Antoniou V, Skilodimou H. Morphotectonic characteristics of Lefkas Island
369 during the Quaternary (Ionian Sea, Greece). *Geologica Balcanica*. 2009;38:23-33.

370 3. Benetatos C, Kiratzi A, Roumelioti Z, Stavrakakis G, Drakatos G, Latoussakis I. The 14
371 August 2003 Lefkas Island (Greece) earthquake: Focal mechanisms of the mainshock and
372 of the aftershock sequence. *Journal of Seismology*. 2005;9(2):171-190.

373 4. Bornovas J. Géologie de l'île de Lefkade. *Geol. and Geophys. Research (I.G.S.R.)*.
374 1964;10:142pp.

- 375 5. Brooks M, Ferentinos G. Tectonics and sedimentation in the Gulf of Corinth and the
376 Zakynthos and Kefallinia channels, western Greece. *Tectonophysics*. 1984;101: 25–54.
- 377 6. Chiarabba C, Frepoli A. Minimum 1D velocity models in Central and Southern Italy: a
378 contribution to better constrain hypocentral determinations. *Ann. Geophys.* 1997;40(4):937-
379 954.
- 380 7. Cisternas, A., Polat, O. and Rivera, L.,. The Marmara Sea Region: Seismic behaviour in
381 time and the likelihood of another large earthquake near Istanbul (Turkey), *Journal of*
382 *Seismology*. 2004; 8:427-437.
- 383 8. D'Alessandro A, Papanastassiou D. Baskoutas I. Hellenic Unified Seismological Network:
384 an evaluation of its performance through SNES method, *Geophys. J. Int.* 2011;185, 1417–
385 1430.
- 386 9. Ganas, A., Oikonomou, I. and Tsimi, C. (2013). NOAfaults: a digital database for active
387 faults in Greece. *Bulletin of the Geological Society of Greece*. 2013; 47(2): 518-530.
388 [doi:http://dx.doi.org/10.12681/bgsg.11079](http://dx.doi.org/10.12681/bgsg.11079)
- 389 10. Gurbuz, C., Aktar, M., Eyidogan, H., Cisternas, A., Haessler, H., Barka, A., Ergin, M.,
390 Turkelli, N., Polat, O., Ucer, S.B. et al. On seismotectonics of the Marmara region (Turkey):
391 Results from a microseismic experiment, *Tectonophysics* 2000; 316: 1-17.
- 392 11. Hatzfeld D, Karakostas V, Ziazia M, Selvaggi G, Leborgne S, Berge C, et al. The Kozani-
393 Grevena (Greece) earthquake of May 13, 1995, a seismological study, *Journal of*
394 *Geodynamics*. 1998 26 (2–4):245-254.
- 395 12. Jacobshagen VH. *Geologie von Griechenland*. Beiträge zur regionalen Geologie der
396 Erde 19. Berlin. 1986.
- 397 13. Kahle HG, Muller MV, Veis G. Trajectories of crustal deformation of western Greece from
398 GPS observations 1989–1994. *Geophys. Res. Lett.* 1996;23(6):677–680.
- 399 14. Karakitsios V, Rigakis N. Evolution and petroleum potential of Western Greece. *J. Pet.*
400 *Geol.* 2007;30:197–218.
- 401 15. Karakostas V, Papadimitriou E. Fault complexity associated with the 14 August 2003
402 Mw6.2 Lefkas, Greece, aftershock sequence. *Acta Geophys.* 2010;58(5):838–854.
- 403 16. Karakostas V, Papadimitriou E, Mesimeri M, Gkarlaouni C, Paradisopoulou P. The 2014
404 Kefalonia doublet (Mw6.1 and Mw6.0), central Ionian islands, Greece: seismotectonic
405 implications along the Kefalonia transform fault zone. *Acta Geotech.* 2014:1–16
406 <http://dx.doi.org/10.2478/s11600-014-0227-4>.
- 407 17. Karakonstantis A. 3-D simulation of crust and upper mantle structure in the broader
408 Hellenic area through Seismic Tomography. Dissertation, National and Kapodistrian
409 University of Athens. 2017. Greek
- 410 18. Kaviris G, Papadimitriou P, Makropoulos K. Magnitude Scales in Central Greece. *Bull.*
411 *Geol. Soc. Greece*. 2007;XXX(3):1114-1124.
- 412 19. Kissling E, Ellworth WL, Eberhart-Phillips D, Kradolfer U. Initial reference models in local
413 earthquake tomography, *Journal of Geophysical Research*. 1994;99:19635–19646.

- 414 20. Klein FW. Users guide to HYPOINVERSE-2000: A Fortran program to solve for
415 earthquake locations and magnitudes. U.S. Geol. Surv. Open-File Rept. 02-171, version 1.0.
416 2002. Available: <https://pubs.usgs.gov/of/2002/0171/pdf/of02-171.pdf>
- 417 21. Kouskouna V, Makropoulos KC, Tsiknakis K. Contribution of historical information to a
418 realistic seismicity and hazard assessment of an area. The Ionian Islands earthquakes of
419 1767 and 1769: historical investigation. In: Stucchi, M. (Ed.), "Historical Investigation of
420 European Earthquakes," Materials of the CEC project "Review of Historical Seismicity in
421 Europe". 1993;(1):195–206.
- 422 22. Kokinou E, Kamberis E, Vafidis A, Monopolis D, Ananiadis G, Zelilidis A. Deep seismic
423 reflection data from offshore western Greece: A new crustal model for the Ionian Sea,
424 Journal of Petroleum Geology. 2005;28(2):185-202.
- 425 23. Lagios E, Sakkas V, Papadimitriou P, Damiata BN, Parcharidis I, Chousianitis K, et al.
426 Crustal deformation in the Central Ionian Islands (Greece): results from DGPS and DInSAR
427 analyses (1995-2006). Tectonophysics. 2007;444:119–145.
- 428 24. Lekkas E, Danamos G, Lozios S. Neotectonic structure of Lefkas Island, Bull. Geol. Soc.
429 Greece, XXXIV. 2001;(1):157-163.
- 430 25. Lopes AEV, Assumpção M. Genetic Algorithm Inversion of the Average 1D Crustal
431 Structure using Local and Regional Earthquakes. Computers & Geosciences.
432 2011;doi:10.1016/j.cageo.2010.11.006.
- 433 26. Makropoulos KC, Kouskouna V. The Ionian Islands earthquakes of 1767 and 1769:
434 seismological aspects. Contribution of historical information to a realistic seismicity and
435 hazard assessment of an area. In: Albin, P., Moroni, A. (Eds.). "Historical Investigation of
436 European Earthquakes," Materials of the CEC Project "Review of Historical Seismicity in
437 Europe". 1994;2:27–36.
- 438 27. Makropoulos K, Kaviris G, Kouskouna V. An updated and extended earthquake
439 catalogue for Greece and adjacent areas since 1900, Nat. Hazards Earth Syst. Sci.
440 2012;12:1425-1430.
- 441 28. Margaris B, Papaioannou C, Theodulidis N, Savvaidis A, Anastasiadis A, Klimis N, et al.
442 "Preliminary Observations on the August 14, 2003 Lefkas Island (Western Greece)
443 Earthquake", EERI Special Earthquake Report, November, (Joint report by Institute of
444 Engineering Seismology and Earthquake Engineering, National Technical University of
445 Athens & University of Athens. 2003:1-12.
- 446 29. Papadimitriou P, Kaviris G, Makropoulos K. The $M_w = 6.3$ 2003 Lefkas Earthquake
447 (Greece) and induced stress transfer changes, Tectonophysics. 2006;423:73–82.
- 448 30. Papadimitriou P, Chousianitis K, Agalos A, Moshou A, Lagios E, Makropoulos K. The
449 spatially extended 2006 April Zakynthos (Ionian Islands, Greece) seismic sequence and
450 evidence for stress transfer. Geophys. Jour. Intern. 2012;190(2):1025-1040.
- 451 31. Pavlides S., Caputo R., Sboras S., Chatzipetros A., Papathanasiou G. and Valkaniotis S.
452 (2010). The Greek catalogue of active faults and database of seismogenic sources, Bulletin
453 of the Geological Society of Greece. 2010; XLIII (1): 486-494.

- 454 32. Polat O., Haessler, H., Cisternas, A., Philip, H., Eyidogan, H., Aktar, M., Frogneux, M.,
455 Comte, D. and Gurbuz, C., 2002b. The Izmit (Kocaeli) Turkish earthquake of August 17,
456 1999: Previous seismicity, aftershocks and seismotectonics, *Bulletin Seismological Society*
457 *of America* 92 (1), 361-375.
- 458 33. Polat O., Haessler, H., Cisternas, A., Philip, H. and Eyidogan, H., 2002a. Analysis and
459 interpretation of the aftershock sequence of the August 17, 1999, Izmit (Turkey) earthquake,
460 *Journal of Seismology* 6, 287-306.
- 461 34. Polat, O., Gok, E. and Yilmaz, D., 2008. Earthquake Hazard of Aegean Extension
462 Region, Turkey, *Turkish Journal of Earth Sciences* 17, 593-614.
- 463 35. Renz C. Die vorneogene stratigraphie der normalsedimentaren Formationen
464 Griechenlands, Greece. Inst. Geol. Subsurf. Res. Athenes. 1955;1-637.
- 465 36. Sakkas V, Lagios E, 2015. Fault modelling of the early-2014 ~M6 Earthquakes in
466 Cephalonia Island (W. Greece) based on GPS measurements. *Tectonophysics*. 2015: 644–
467 645, 184–196. <http://dx.doi.org/10.1016/j.tecto.2015.01.010>.
- 468 37. Scordilis EM, Karakaisis GF, Karacostas BG, Panagiotopoulos DG, Comninakis PE,
469 Papazachos B.C. Evidence for transform faulting in the Ionian Sea: the Cephalonia island
470 earthquake sequence of 1983. *PAGEOPH*. 1985;123:387–397.
- 471 38. Stucchi M, Rovida A, Gomez Capera AA, Alexandre P, Camelbeeck T, Demircioglu MB,
472 et al. The SHARE European Earthquake Catalog (SHEEC) 1000–1899. *J. Seismolog.*
473 2013;17(2):523–544.
- 474 39. Toda S, Stein RS, Richards-Dinger K, Bozkurt S. Forecasting the evolution of seismicity
475 in southern California: Animations built on earthquake stress transfer. *J. Geophys. Res.*
476 2005;B05S16, doi:10.1029/2004JB003415.
- 477 40. Toda S, Stein R, Lin J, Sevilgen V. Coulomb 3.2, Graphic-rich deformation & stress-
478 change software. User Guide. 2010.
- 479 41. Triantaphyllou MV. Calcareous nannofossil biostratigraphy of Langhian deposits in
480 Lefkas (Ionian Islands). *Bulletin of the Geological Society of Greece. Proceedings of the 12th*
481 *International Congress, 2010;XLII(2):754-762.*
- 482 42. Twiss RJ, Moores EM. *Structural Geology*. W.H. Freeman and Company, New York;
483 1992.
- 484 43. van Hinsbergen DJJ, van der Meer DG, Zachariasse WJ, et al. *Int J Earth Sci (Geol*
485 *Rundsch)*. 2006: 95: 463. <https://doi.org/10.1007/s00531-005-0047-5>.
- 486 44. Zahradnik J, Serpetsidaki A, Sokos E, Tselentis GA. Iterative Deconvolution of Regional
487 Waveforms and a Double-Event Interpretation of the 2003 Lefkas Earthquake, Greece. *Bull.*
488 *Seism. Soc. Am.* 2005;95(1):159–172.
- 489 45. Zelilidis A, Kontopoulos N, Piper DJW, Avramidis P. Tectonic and sedimentological
490 evolution of the Pliocene-Quaternary basins of Zakynthos Island, Greece: Case study of the
491 transition from compressional to extensional tectonics. *Basin Research*. 1998;10:393-408.
492